Same-Sign Dilepton Signature in the Inert Doublet Model

Zhi-Long Han

School of Physics and Technology, University of Jinan

July 20, 2021

Based on CPC(2021) 073114, arXiv:2101.06862

Introduction

- Particle Dark Matter – WIMPs are the best-motivated candidates.

  ✠ Scalar Singlet [1306.4275] ⋆ Inert Doublet [0906.1609]

- IDM – SM Higgs Doublet + Inert Higgs Doublet(Z_2 symmetry)

  ⁕ $h,\ H^{\pm}, A, H$(DM)

- Parameter Space of IDM – relic density, direct, indirect detection,...
  - Low mass region: 55$\sim$75 GeV
  - High mass region: $>$500 GeV
- Collider Signature of IDM :
  - LHC: dilepton [0909.3094], trilepton [1005.0090]
  - e^+e^- collider: dilepton [1811.06952]

Motivation

Production of $H^{\pm}H^{\pm}$ via VBF at LHC [1906.09101]

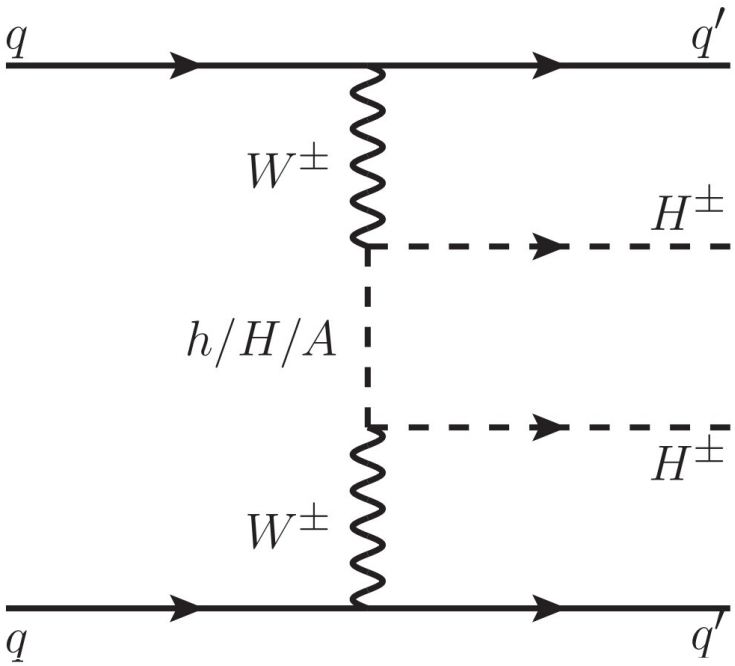

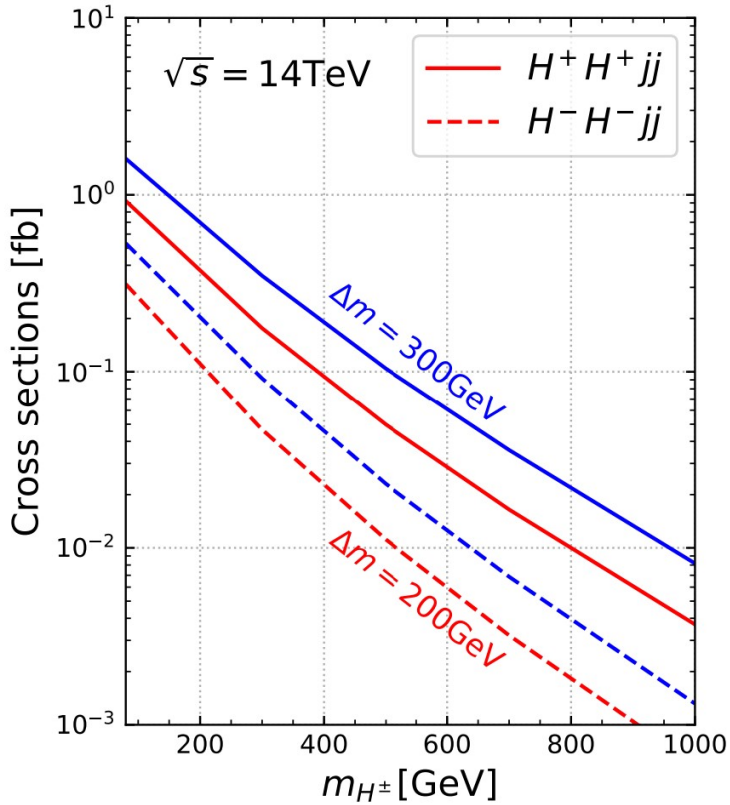

At high energies $\sqrt{s} \gg M_W$, the amplitude is

$$\mathcal{M}(W^{\pm}W^{\pm} \to H^{\pm}H^{\pm}) \simeq 2(m_A^2 - m_H^2)/v^2$$

The Inert Doublet Model

SM Higgs doublet H_1 + an inert Higgs doublet H_2

$$H_1 = \begin{pmatrix} G^+ \\ \frac{1}{\sqrt{2}}(v + h + iG^0) \end{pmatrix}, \quad H_2 = \begin{pmatrix} H^+ \\ \frac{1}{\sqrt{2}}(H + iA) \end{pmatrix}, \tag{1}$$

The Higgs potential under the exact Z_2 symmetry is

$$\begin{aligned} V &= \mu_1^2 H_1^\dagger H_1 + \mu_2^2 H_2^\dagger H_2 + \lambda_1 (H_1^\dagger H_1)^2 + \lambda_2 (H_2^\dagger H_2)^2 + \lambda_3 (H_1^\dagger H_1)(H_2^\dagger H_2) \\ &\quad + \lambda_4 (H_1^\dagger H_2)(H_2^\dagger H_1) + \frac{\lambda_5}{2}\left[(H_1^\dagger H_2)^2 + \text{h.c.}\right]. \end{aligned} \tag{2}$$

Masses of scalars are

$$m_h^2 = -2\mu_1^2 = 2\lambda_1 v^2 \quad , \quad m_H^2 = \mu_2^2 + \frac{1}{2}(\lambda_3 + \lambda_4 + \lambda_5)v^2 \tag{3}$$

$$m_{H^\pm}^2 = \mu_2^2 + \frac{1}{2}\lambda_3 v^2 \quad , \quad m_A^2 = \mu_2^2 + \frac{1}{2}(\lambda_3 + \lambda_4 - \lambda_5)v^2 \tag{4}$$

Free parameters set $\{m_H, m_A, m_{H^\pm}, \lambda_2, \lambda_L\}$, $\lambda_L = (\lambda_3 + \lambda_4 + \lambda_5)/2$

Constraints

- **Perturbativity:**

$$|\lambda_1, \lambda_2, \lambda_3, \lambda_4, \lambda_5| \leq 4\pi. \tag{5}$$

- **Vacuum stability:**

$$\lambda_1 > 0, \lambda_2 > 0, \lambda_3 + 2\sqrt{\lambda_1 \lambda_2} > 0, \lambda_3 + \lambda_4 - |\lambda_5| + 2\sqrt{\lambda_1 \lambda_2} > 0. \tag{6}$$

- **Global minimum:**

$$\frac{\mu_1^2}{\sqrt{\lambda_1}} \leq \frac{\mu_2^2}{\sqrt{\lambda_2}}. \tag{7}$$

- **Unitarity:** valid up to about 10 TeV [1503.03085]

$$m_A - m_H \lesssim 300 \text{ GeV}, \; m_{H^\pm} - m_H \lesssim 300 \text{ GeV}. \tag{8}$$

- **Electroweak precision tests:**

$$S = 0.06 \pm 0.09, \; T = 0.01 \pm 0.07, \tag{9}$$

with correlation coefficient +0.91.

Constraints

- **Gauge boson widths:**

$$m_{A,H} + m_{H^\pm} > m_W,\ m_A + m_H > m_Z,\ 2m_{H^\pm} > m_Z. \tag{10}$$

- **Collider searches:** supersymmetric particles at LEP

$$m_A \leq 100\ \text{GeV},\ m_H \leq 80\ \text{GeV},\ m_A - m_H \geq 8\ \text{GeV} \tag{11}$$

when the above conditions are satisfied simultaneously.

$$m_{H^\pm} \geq 70\ \text{GeV} \tag{12}$$

⁎Dilepton and trilepton signal at LHC

$$pp \rightarrow AH \rightarrow ZHH \rightarrow l^+l^- + \not{E}_T \tag{13}$$

$$pp \rightarrow H^\pm A \rightarrow W^\pm H + ZH \rightarrow l^\pm l^+ l^- + \not{E}_T \tag{14}$$

Constraints

- **SM Higgs data:** When $m_H < m_h/2$, Higgs invisible decay $h \to HH$

$$\text{BR}(h \to \text{invisible}) < 0.24. \tag{15}$$

The charged scalar $H^\pm$ will also impact $h \to \gamma\gamma$

$$\mu_{\gamma\gamma} = 1.14^{+0.38}_{-0.36}. \tag{16}$$

- **Relic density:** Planck result

$$\Omega h^2 = 0.1200 \pm 0.0012. \tag{17}$$

- **Direct detection:** XENON1T [1805.12562]

We randomly scan the the low mass region

$$m_H \in [50, 80]\ \text{GeV},\ \lambda_L \in [-0.04, 0.04],\ \lambda_2 \in [0, 1] \tag{18}$$
$$m_A - m_H \in [0, 300]\ \text{GeV},\ m_{H^\pm} - m_H \in [0, 300]\ \text{GeV}$$

DM Parameter Space in Low Mass Region

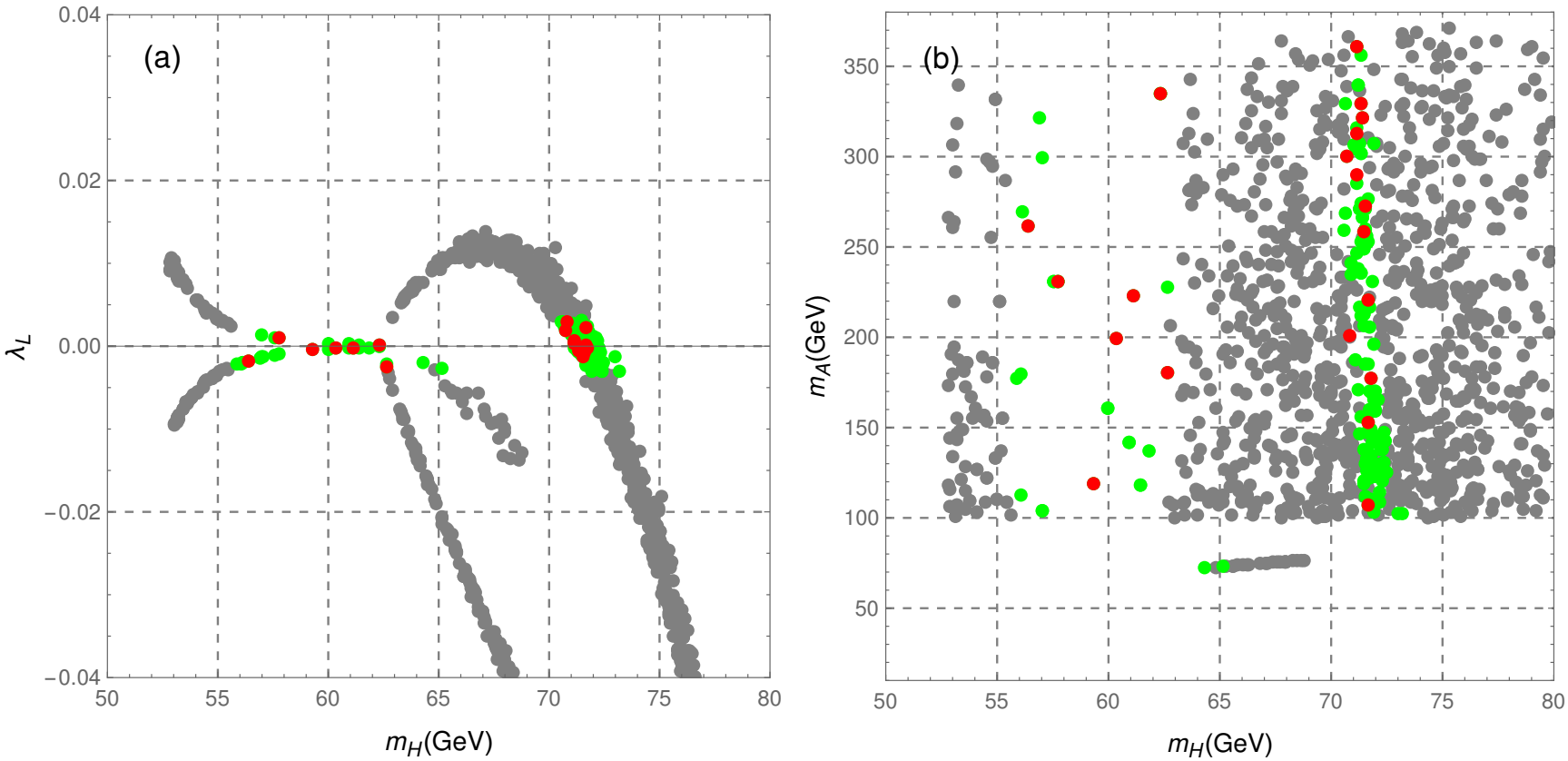

The gray points satisfy the constraints discussed from Eqn 5 to Eqn 17, but are excluded by XENON1T. The green and red points are allowed by all constraints. The red points are the benchmark points.

DM Parameter Space in Low Mass Region

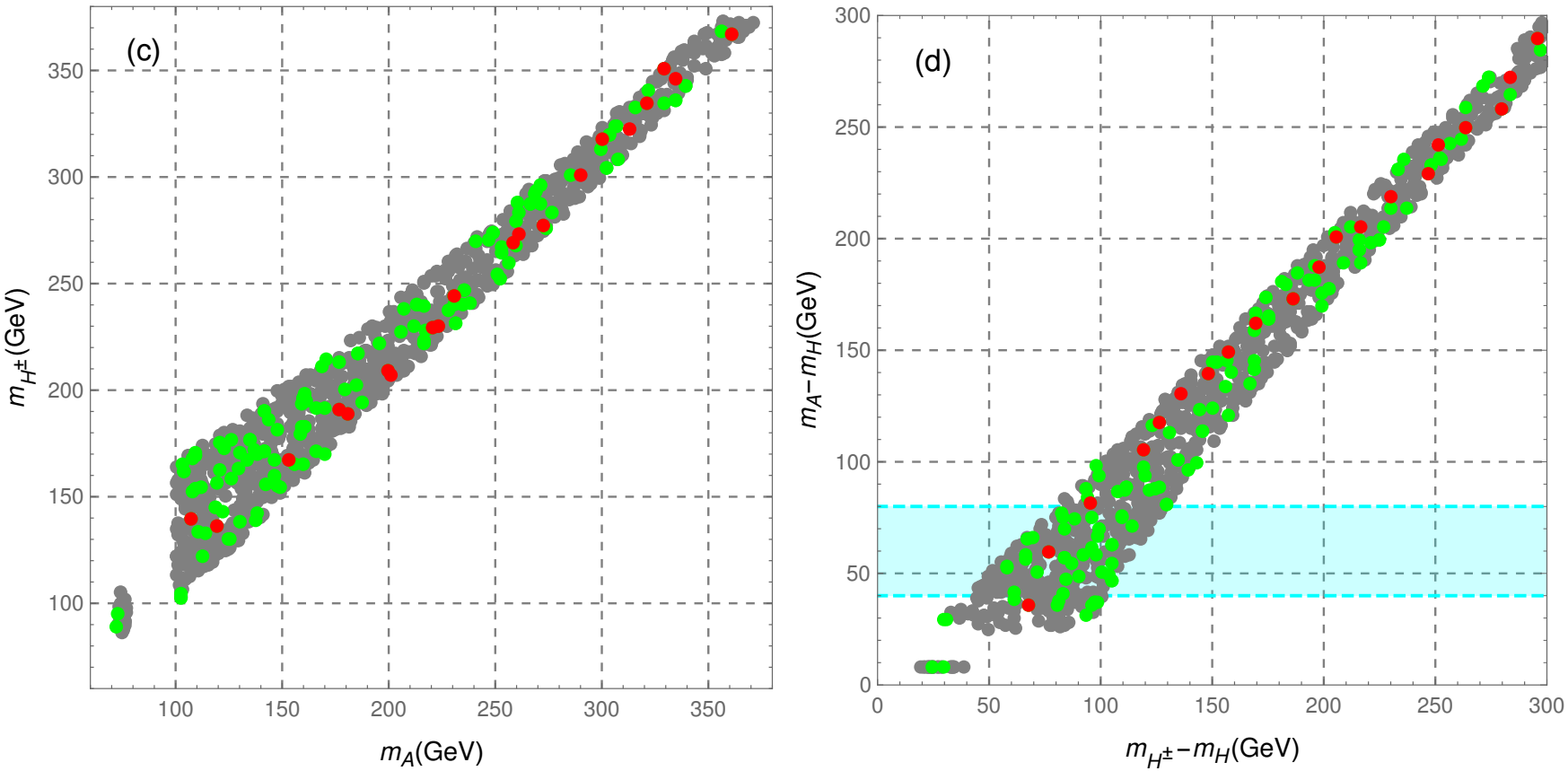

Same as previous figure. The light blue band in panel d corresponds to the promising region of the opposite-sign dilepton signature.

DM Benchmark Points

No.	m_H(GeV)	m_A(GeV)	$m_{H^\pm}$(GeV)	λ_2	λ_L	Ωh^2	σ @14TeV (fb)	σ @27TeV (fb)
BP1	71.69	107.5	139.6	0.4097	0.002203	0.1210	0.054	0.160
BP2	59.30	119.1	136.3	0.09806	-0.0004655	0.1213	0.154	0.451
BP3	71.67	152.9	167.0	0.1750	0.0001029	0.1233	0.214	0.657
BP4	71.76	177.0	190.9	0.3855	-0.0002066	0.1180	0.285	0.914
BP5	62.64	180.5	189.1	0.7473	-0.002478	0.1177	0.355	1.139
BP6	70.82	201.1	206.8	0.8602	0.002879	0.1233	0.373	1.232
BP7	60.37	199.7	208.8	0.6200	-0.0002771	0.1210	0.409	1.351
BP8	71.63	220.8	229.1	0.5264	-0.0007215	0.1193	0.399	1.362
BP9	61.12	223.2	230.3	0.4692	-0.0002002	0.1227	0.454	1.553
BP10	57.76	230.7	244.3	0.9192	0.0009435	0.1185	0.454	1.578
BP11	71.44	258.6	269.0	0.6848	-0.0007471	0.1214	0.446	1.616
BP12	71.55	272.6	277.1	0.00294	-0.001236	0.1205	0.483	1.765
BP13	56.40	261.4	273.1	0.5082	-0.001733	0.1191	0.495	1.799
BP14	71.17	290.1	301.2	0.5216	0.0006213	0.1200	0.467	1.788
BP15	70.72	299.9	317.8	0.7495	0.001944	0.1235	0.451	1.755
BP16	71.12	312.9	322.7	0.04812	0.0002456	0.1221	0.482	1.892
BP17	71.39	321.4	334.9	0.7437	-0.0001886	0.1172	0.468	1.883
BP18	71.31	329.1	350.8	0.1182	-0.0005298	0.1204	0.441	1.813
BP19	62.32	334.6	346.0	0.2196	0.0001064	0.1180	0.498	2.037
BP20	71.14	360.8	366.8	0.1079	0.0005207	0.1192	0.495	2.087

σ denotes the cross section of $pp \to H^\pm H^\pm jj$ with preselection cuts

$$\eta_{j_1} \times \eta_{j_2} < 0, \ |\Delta\eta_{jj}| > 2.5. \tag{19}$$

Production Cross Section

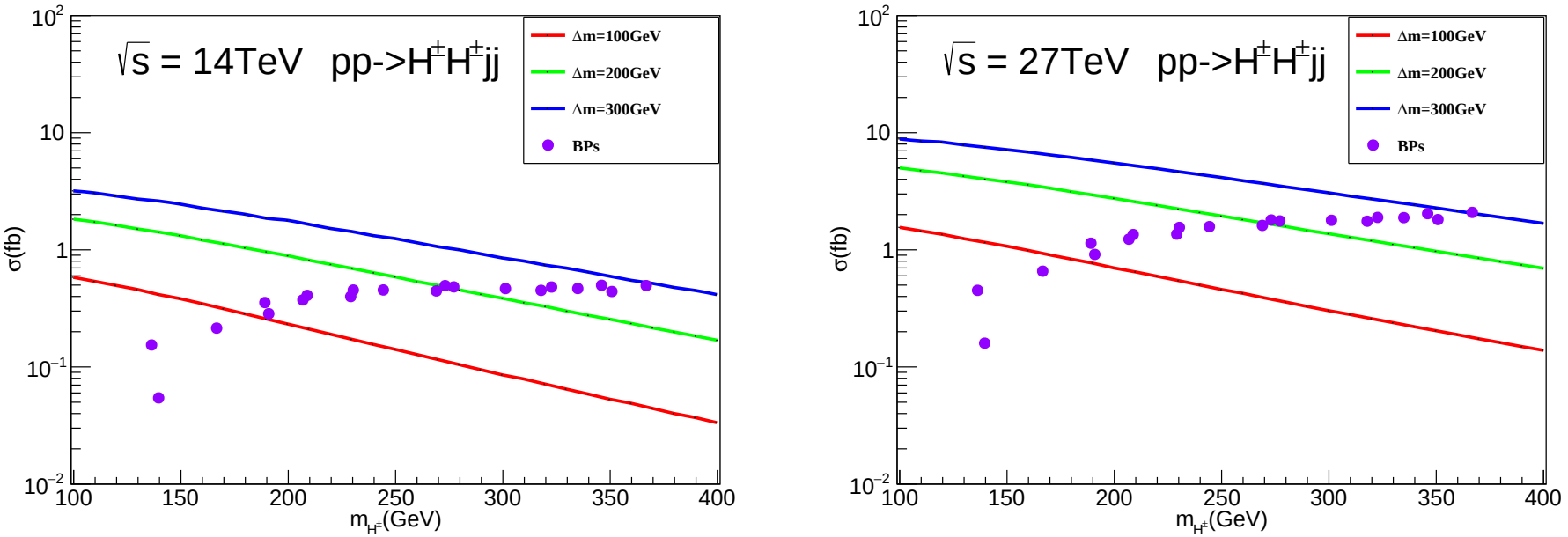

Figure: Production cross section of process $pp \to H^{\pm}H^{\pm}jj$ at the $\sqrt{s} = 14$ TeV HL-LHC (left panel) and the $\sqrt{s} = 27$ TeV HE-LHC (right panel) as a function of $m_{H^{\pm}}$ with $\Delta m =$ 100GeV, 200GeV, 300GeV, respectively. Here, we also fix $m_H = 62$ GeV.

The same-sign dilepton signature

$$pp \to H^{\pm}H^{\pm}jj \to (W^{\pm}H)(W^{\pm}H)jj \to (l^{\pm}\nu)H(l^{\pm}\nu)Hjj \to l^{\pm}l^{\pm}\not{E}_T jj \quad (20)$$

Branching Ratio of $H^{\pm}$

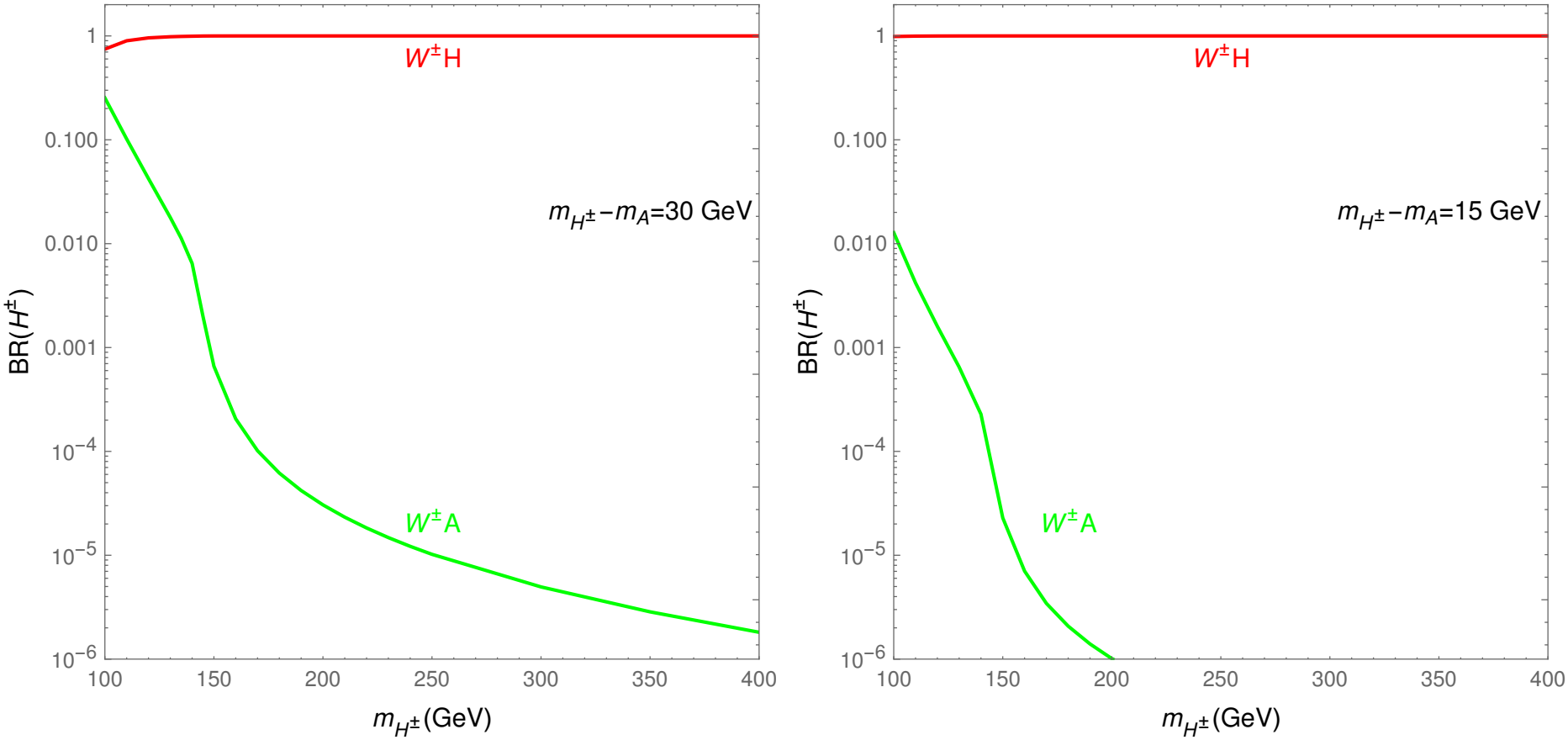

Figure: Branching ratio of the charged scalar $H^{\pm}$ for $m_{H^{\pm}} - m_A = 30$ GeV (left panel) and $m_{H^{\pm}} - m_A = 15$ GeV (right panel), where m_H is fixed to be 62 GeV in both cases. The package **2HDMC** is used for calculating these branching ratios.

Distribution of P_T^l and ΔP_T at LHC

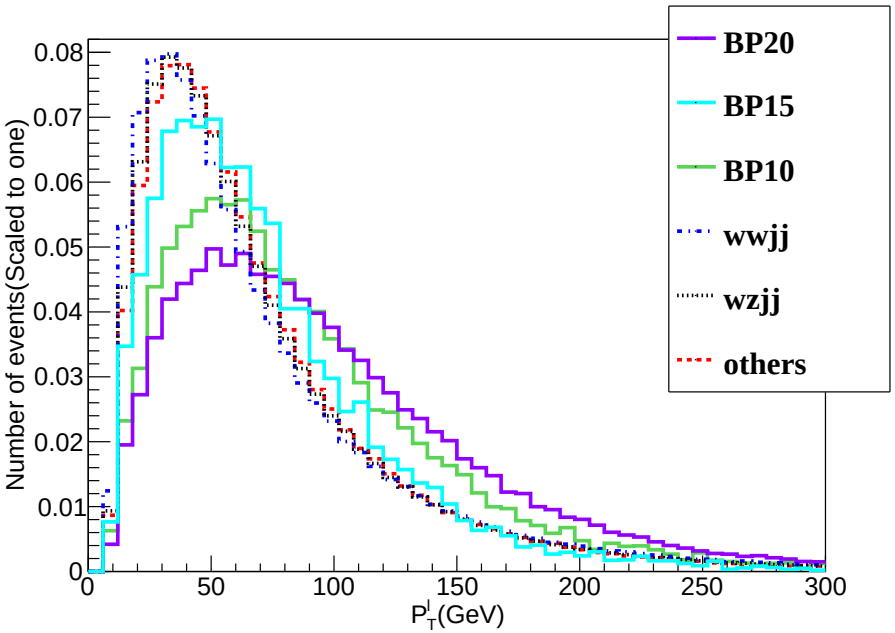

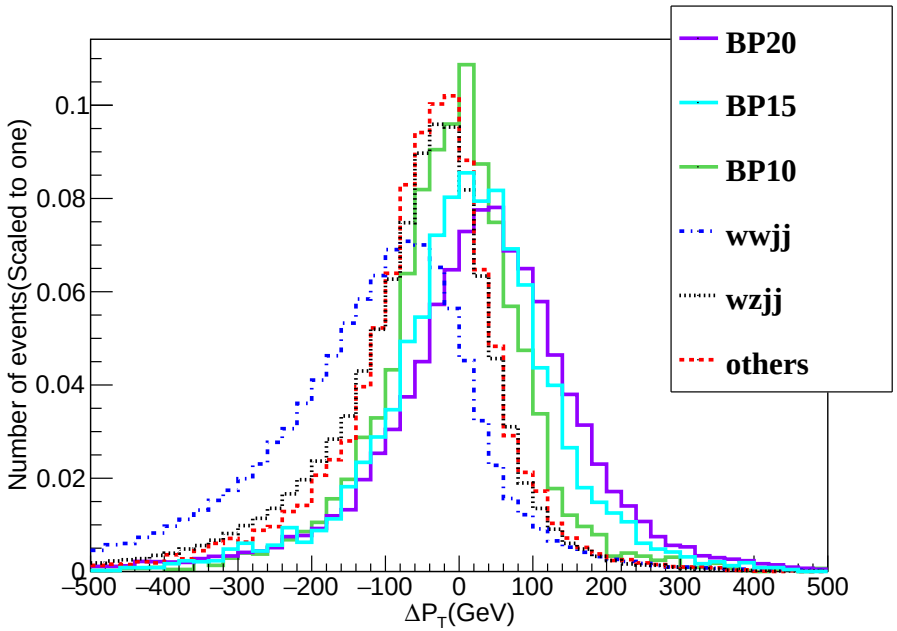

ΔP_T is defined as $\Delta P_T = (P_T^{l_1} + P_T^{l_2}) - (P_T^{j_1} + P_T^{j_2})$

- Cuts-1 on the same-sign dilepton

$$N(l^{\pm}) = 2, P_T^{l^{\pm}} > 20 \text{ GeV}, |\eta_{l^{\pm}}| < 2.5, \tag{21}$$

- Cuts-2 on the forward jet pair

$$N(j) \geq 2, P_T^j > 30 \text{ GeV}, |\eta_j| < 5, N(b) = 0. \tag{22}$$

Distribution of $\overline{\Delta\eta_{jl}}$ and z_l^* at LHC

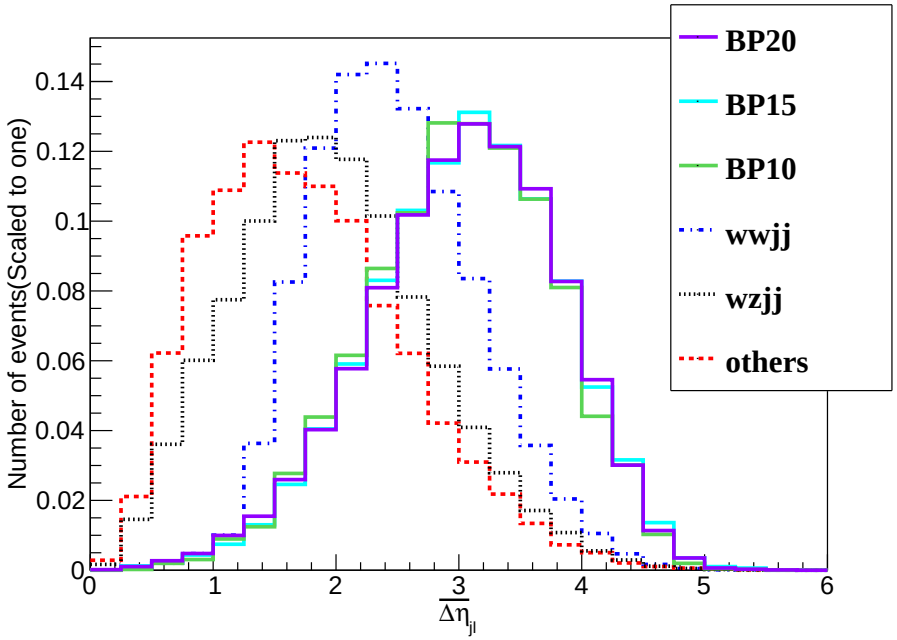

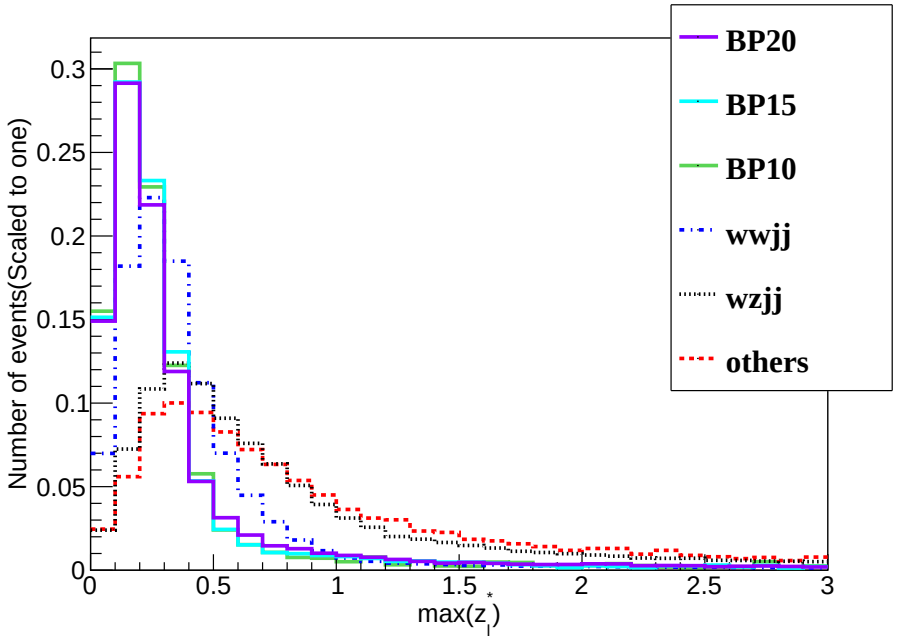

$\overline{\Delta\eta_{jl}}$ and z_l^* are defined as

$$\overline{\Delta\eta_{jl}} = \sqrt{\sum_{m=1}^{2}\sum_{n=1}^{2}\frac{(\eta_{jm}-\eta_{ln})^2}{4}}, z_l^* = \left|\eta_l - \frac{\eta_{j1}+\eta_{j2}}{2}\right| / |\eta_{j1}-\eta_{j2}|. \quad (23)$$

Distribution of $\not{E}_T$ and M_{T2} at LHC

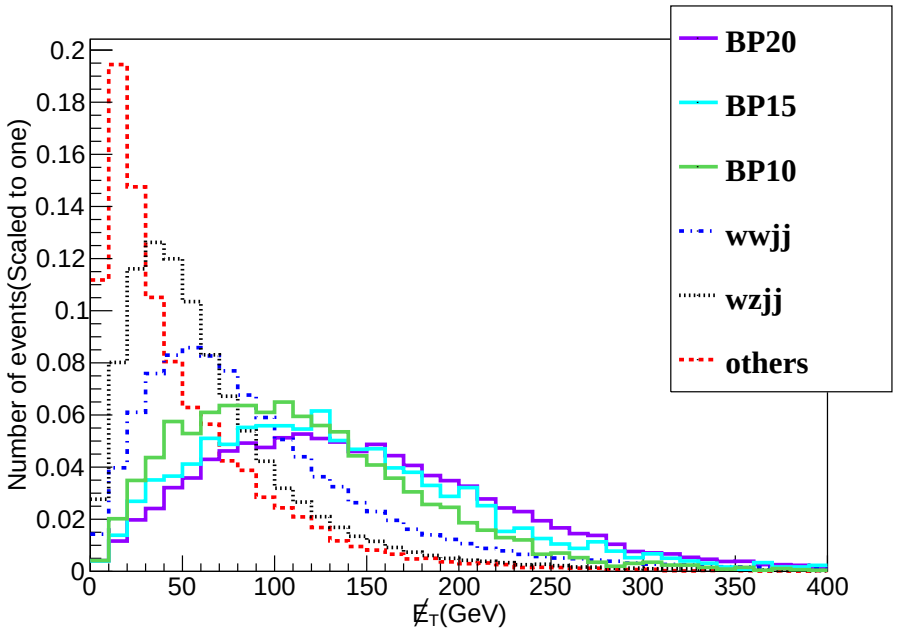

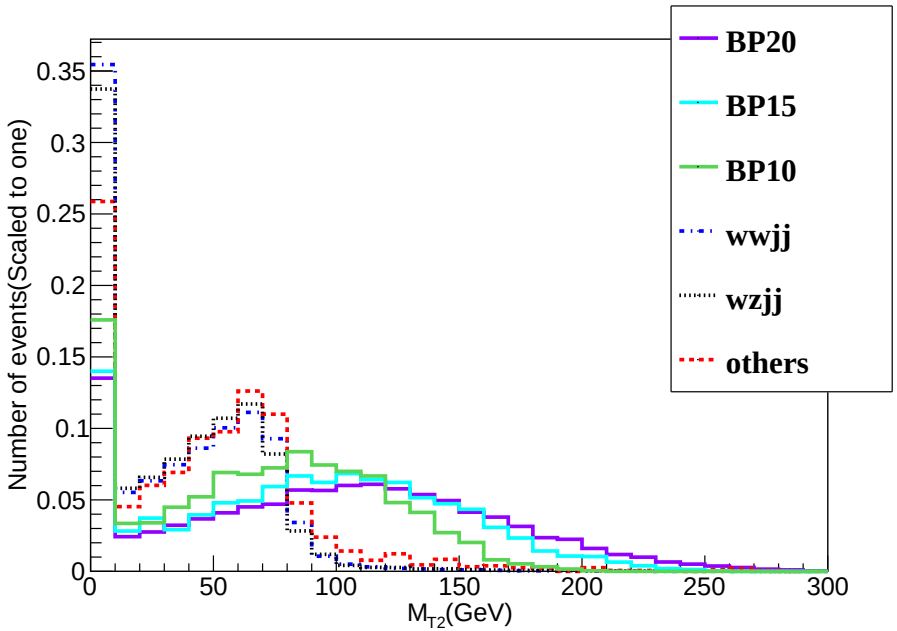

- Cuts-3 we adopted are

$$\Delta P_T > 0,\ \overline{\Delta\eta_{jl}} > 3,\ \max(z_l^*) < 0.3. \tag{24}$$

- Cuts-4 we adopted are

$$\not{E}_T > 100\ \text{GeV},\ M_{T2} > 100\ \text{GeV}. \tag{25}$$

Cut Flow Table for HL-LHC

Cross section (fb)	BP10	BP15	BP20	$W^{\pm}W^{\pm}jj$	$WZjj$	Others
Preselection	1.88×10^{-2}	1.89×10^{-2}	2.04×10^{-2}	1.35×10^{1}	5.50×10^{1}	3.05×10^{0}
$N(l^{\pm}) = 2, P_T^{l^{\pm}} > 20$ GeV						
$\lvert\eta_{l^{\pm}}\rvert < 2.5$	1.01×10^{-2}	1.08×10^{-2}	1.19×10^{-2}	5.29×10^{0}	6.43×10^{0}	3.66×10^{-1}
$N(j) \geq 2, P_T^{j} > 30$ GeV						
$\lvert\eta_j\rvert < 5, N(b) = 0$	8.62×10^{-3}	9.13×10^{-3}	1.02×10^{-2}	4.60×10^{0}	5.43×10^{0}	2.05×10^{-1}
$\Delta P_T > 0, \overline{\Delta\eta_{jl}} > 3$						
$\max(z_l^*) < 0.3$	1.56×10^{-3}	2.48×10^{-3}	3.06×10^{-3}	1.34×10^{-1}	2.834×10^{-2}	1.12×10^{-3}
$\not{E}_T > 100$ GeV						
$M_{T2} > 100$ GeV	3.71×10^{-4}	8.41×10^{-4}	1.33×10^{-3}	7.31×10^{-4}	1.10×10^{-4}	8.87×10^{-5}
Significance	0.67	1.52	2.39	—	—	—

Table: Cut flow table for BP10, BP15, BP20 signal and various background process at $\sqrt{s} = 14$ TeV. The significance $S/\sqrt{B}$ is calculated by assuming an integrated luminosity $\mathcal{L} = 3$ ab^{-1}.

Distribution of $\not{E}_T$ and M_{T2} at HE-LHC

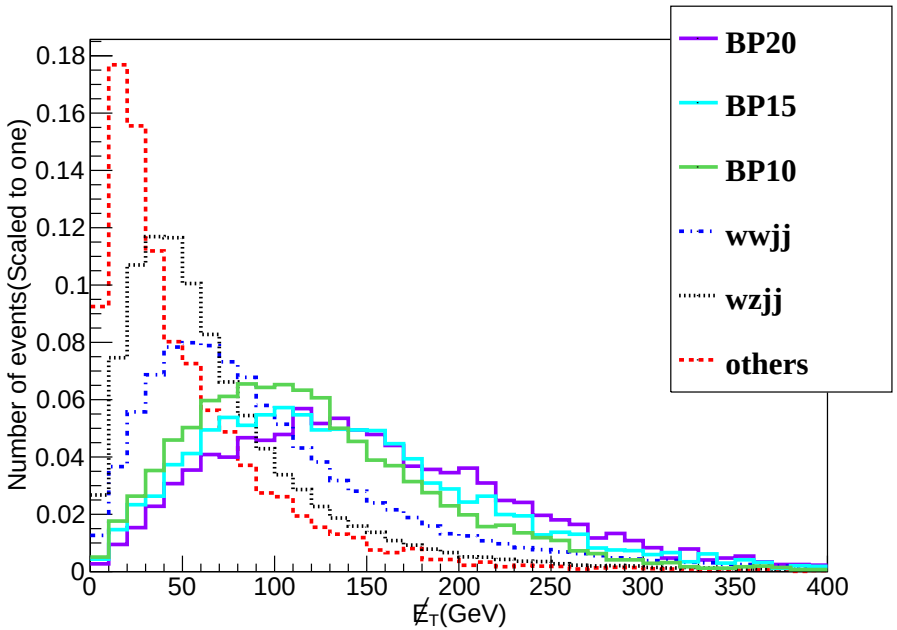

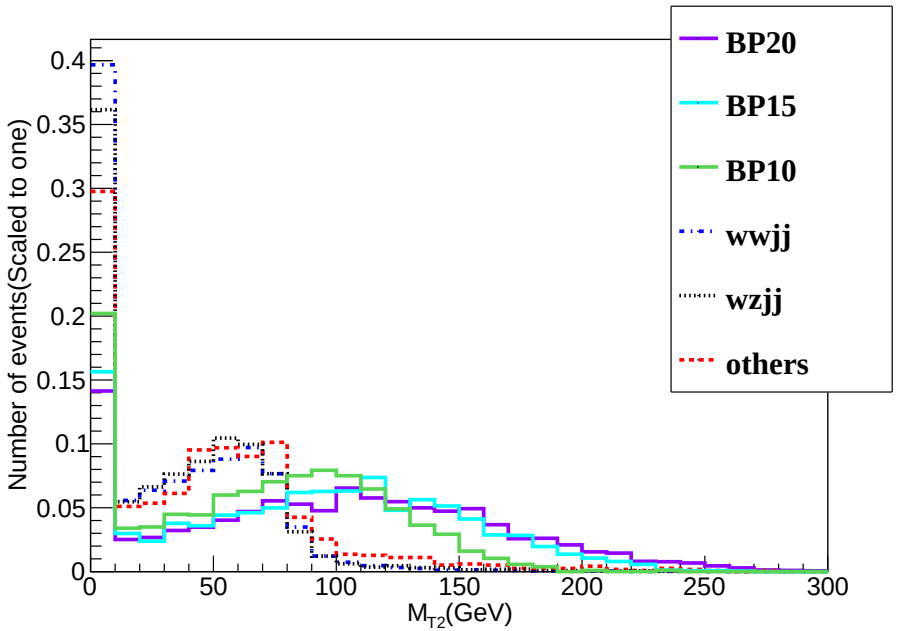

We adopt the same criteria as 14 TeV for cuts-1 to cuts-3. Meanwhile we slightly tight cuts-4 as

$$\not{E}_T > 110 \text{ GeV}, \ M_{T2} > 125 \text{ GeV}. \tag{26}$$

Cut Flow Table for HE-LHC

Cross section(fb)	BP10	BP15	BP20	$W^{\pm}W^{\pm}jj$	$WZjj$	Others
Preselection	6.57×10^{-2}	7.40×10^{-2}	8.59×10^{-2}	4.61×10^{1}	1.95×10^{2}	1.38×10^{1}
$N(l^{\pm}) = 2, P_T^{l^{\pm}} > 20$ GeV						
$\lvert\eta_{l^{\pm}}\rvert < 2.5$	3.19×10^{-2}	3.77×10^{-2}	4.54×10^{-2}	1.47×10^{1}	1.95×10^{1}	1.32×10^{0}
$N(j) \geq 2, P_T^{j} > 30$ GeV						
$\lvert\eta_j\rvert < 5, N(b) = 0$	2.49×10^{-2}	3.06×10^{-2}	3.74×10^{-2}	1.13×10^{1}	1.58×10^{1}	8.67×10^{-1}
$\Delta P_T > 0, \overline{\Delta\eta_{jl}} > 3$						
$\max(z_l^*) < 0.3$	6.13×10^{-3}	9.74×10^{-3}	1.23×10^{-2}	4.94×10^{-1}	1.21×10^{-1}	4.33×10^{-3}
$\not{E}_T > 110$ GeV						
$M_{T2} > 125$ GeV	5.58×10^{-4}	2.09×10^{-3}	3.72×10^{-3}	2.79×10^{-3}	3.90×10^{-4}	0
Significance	1.21	4.54	8.08	—	—	—

Table: Cut flow table for BP10, BP15, BP20 signal and various background process at $\sqrt{s} = 27$ TeV. The significance $S/\sqrt{B}$ is calculated by assuming an integrated luminosity $\mathcal{L} = 15$ ab^{-1}.

Significance of 20 BPs

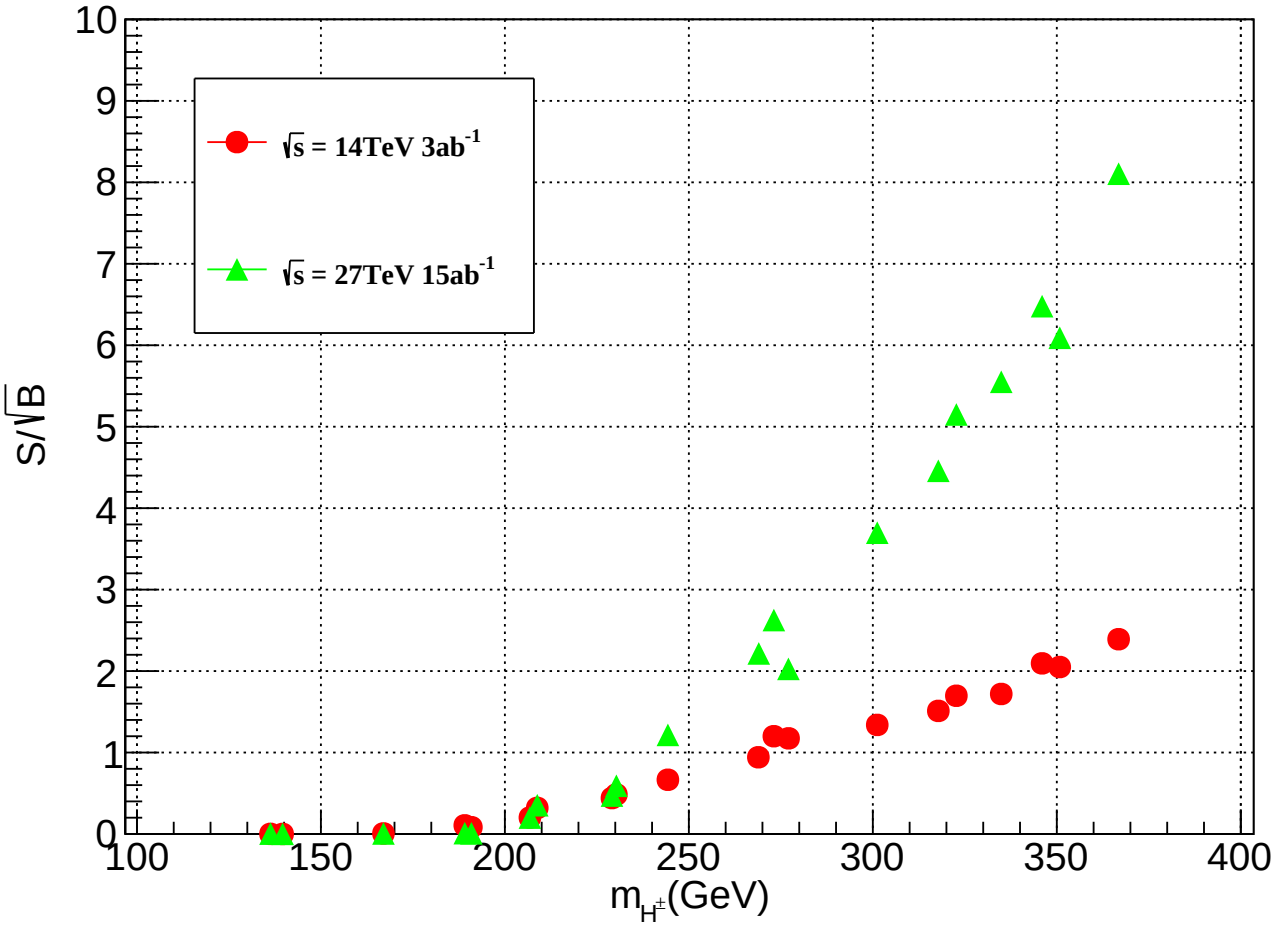

Figure: Significance of all twenty BPs at $\sqrt{s} = 14$ TeV, $\mathcal{L} = 3$ ab^{-1}(red points) and $\sqrt{s} = 27$ TeV, $\mathcal{L} = 15$ ab^{-1}(green points).

Conclusion

- We perform a random scan over the low mass region of IDM, and find three viable parameter space
  $m_H \lesssim m_h/2$, $m_H \sim 71.5$ GeV, $m_A - m_H \sim 8$ GeV with $m_H \sim 65$ GeV
- $\not{E}_T$ and M_{T2} are efficient cuts to suppress background.
- The same-sign dilepton signature is not promising at $\sqrt{s} = 14$ TeV HL-LHC
- This signature is promising at $\sqrt{s} = 27$ TeV with the viable region

$$250 \text{ GeV} \lesssim m_{H^\pm} - m_H \lesssim 300 \text{ GeV}$$

- This signature is promising for large mass splitting $\Delta m = m_A - m_H$, which is complementary to the well studied opposite-sign dilepton signature.